




Pharmacokinetics and Efficacy of the Benzothiazinone BTZ-043 against Tuberculous Mycobacteria inside Granulomas in the Guinea Pig Model

Emmelie Eckhardt,^a Yan Li,^b Svenja Mamerow,^c Jan Schinköthe,^d Julia Sehl-Ewert,^a Julia Dreisbach,^{e,f} Björn Corleis,^a Anca Dorhoi,^a Jens Teifke,^a Christian Menge,^c Florian Kloss,^b  Max Bastian^a

^aFriedrich-Loeffler-Institut, Federal Research Institute for Animal Health, Greifswald, Germany

^bTransfer Group Anti-infectives, Leibniz Institute for Natural Product Research and Infection Biology, Leibniz-HKI, Jena, Germany

^cFriedrich-Loeffler-Institut, Federal Research Institute for Animal Health, Jena, Germany

^dInstitute of Veterinary Pathology, Faculty of Veterinary Medicine, Leipzig University, Leipzig, Germany

^eDivision of Infectious Diseases and Tropical Medicine, University Hospital of the University of Munich (LMU), Munich, Germany

^fGerman Center for Infection Research (DZIF), Partner Site Munich, Munich, Germany

ABSTRACT Tuberculosis (TB), caused by *Mycobacterium tuberculosis*, is the world's leading cause of mortality from a single bacterial pathogen. With increasing frequency, emergence of drug-resistant mycobacteria leads to failures of standard TB treatment regimens. Therefore, new anti-TB drugs are urgently required. BTZ-043 belongs to a novel class of nitrobenzothiazinones, which inhibit mycobacterial cell wall formation by covalent binding of an essential cysteine in the catalytic pocket of decaprenylphosphoryl- β -D-ribose oxidase (DprE1). Thus, the compound blocks the formation of decaprenylphosphoryl- β -D-arabinose, a precursor for the synthesis of arabinans. An excellent *in vitro* efficacy against *M. tuberculosis* has been demonstrated. Guinea pigs are an important small-animal model to study anti-TB drugs, as they are naturally susceptible to *M. tuberculosis* and develop human-like granulomas after infection. In the current study, dose-finding experiments were conducted to establish the appropriate oral dose of BTZ-043 for the guinea pig. Subsequently, it could be shown that the active compound was present at high concentrations in *Mycobacterium bovis* BCG-induced granulomas. To evaluate its therapeutic effect, guinea pigs were subcutaneously infected with virulent *M. tuberculosis* and treated with BTZ-043 for 4 weeks. BTZ-043-treated guinea pigs had reduced and less necrotic granulomas than vehicle-treated controls. In comparison to the vehicle controls a highly significant reduction of the bacterial burden was observed after BTZ-043 treatment at the site of infection and in the draining lymph node and spleen. Together, these findings indicate that BTZ-043 holds great promise as a new antimycobacterial drug.

KEYWORDS BTZ-043, guinea pig, *Mycobacterium tuberculosis*, *Mycobacterium bovis* BCG, MDR-TB, treatment, new antibiotics

Tuberculosis (TB) in humans is caused by *Mycobacterium tuberculosis* and by other bacteria of the *M. tuberculosis* complex (MTC). TB is the world's leading cause of mortality from a single bacterial pathogen. In 2020, about 10 million people fell ill with TB and about 1.5 million deaths were estimated (1). Although treatment of TB is complicated, consisting of 6 months of treatment with a regimen of four different drugs, 85% of newly diagnosed patients are successfully treated (1). Commercially available antimycobacterial substances can be differentiated into first-line (e.g., rifampicin, isoniazid [INH], and ethambutol) and second-line drugs, which are used in combination to treat TB (2, 3). An increasing problem is the emergence of resistant mycobacteria,

Copyright © 2023 American Society for Microbiology. All Rights Reserved.

Address correspondence to Max Bastian, max.bastian@fli.de.

The authors declare no conflict of interest.

Received 24 October 2022

Returned for modification 7 December 2022

Accepted 16 February 2023

Published 28 March 2023

which are either rifampicin resistant (RR-TB), resistant to rifampicin and isoniazid (MDR-TB), or extensively drug-resistant (XDR-TB). XDR-TB strains are MDR-TB strains which developed an additional resistance to fluoroquinolones and any of the second-line drugs (4). According to the WHO, in 2019, about half a million people developed RR-TB, of whom around 75% were MDR (5). The highest frequency of drug-resistant TB is found in countries of the former Soviet Union, with over 50% of relapse TB cases being MDR-TB. Globally, 3.3% of new and 17.7% of relapse TB cases developed RR- or MDR-TB in 2019 (5). With the increase of drug-resistant TB, appropriate treatment is getting more complicated and expensive. Drug-resistant TB leads to higher mortality rates. Therefore, new treatment approaches and drug regimens have to be developed and tested (6–10).

The structure of their cell wall is unique to mycobacteria, and enzymes involved in cell wall synthesis are therefore prominent targets for current and newly developed anti-TB drugs (11). One of the most promising substances is the benzothiazinone BTZ-043, which was first proposed as an anti-TB drug by Makarov et al. in 2009 (12). BTZ-043 inhibits *M. tuberculosis* cell wall synthesis by blocking decaprenylphosphoryl- β -D-ribose oxidase (DprE1) (13, 14). Consequently, cell wall arabinans cannot be formed, resulting in cell lysis and bacterial death. A very low MIC and good *in vitro* efficacy of BTZ-043 against different mycobacteria and nocardia have been demonstrated (15–17). In combination with other anti-TB drugs, such as rifampicin or isoniazid, benzothiazinones show a promising additive effect; a synergistic effect with bedaquiline is observed *in vitro* (18) and *in vivo* (17). Toxicologically, BTZ-043 showed no negative effects at therapeutic drug levels and no genotoxicity or mutagenicity in rats (19). In studies with BALB/c mice, no adverse effects after single-dose (5 g/kg of body weight) or repeated (25 and 250 mg/kg) treatment with BTZ-043 were observed (12).

Theoretically, a mutation at the Cys387 position of DprE1 could confer resistance against BTZ-043 (11), but all clinical isolates tested in a European study were found to be uniformly susceptible (20). BTZ-043 is currently undergoing phase II clinical trials within a partnership of German academic institutions and involvement of four leading consortia, the German Center for Infection Research (DZIF), the PanACEA consortium, Unite4TB, and InfectControl (21).

Although the compound has already been advanced to clinical phase trials, so far, there are no published studies that elucidate whether BTZ-043 is able to penetrate poorly vascularized granulomatous tissues and exert its antibacterial effect there. Guinea pigs have been long used as animal models to understand and describe TB infection, as they show many features of human TB disease. In particular, upon TB infection they develop necrotizing, caseating granulomas that resemble TB granulomas in human patients (22). To test the effect of BTZ-043 in a TB granuloma model, we made use of our long-standing experience with guinea pigs. In a dose-finding study, the appropriate dose of BTZ-043 for guinea pigs was determined. Subsequently, the level of BTZ-043 in *Mycobacterium bovis* BCG-induced granulomas was assessed. Finally, we investigated the therapeutic effect of BTZ-043 in guinea pigs previously infected with virulent mycobacteria.

RESULTS

Plasma levels of BTZ-043 and its metabolite after oral BTZ-043 administration to guinea pigs. Plasma levels of BTZ-043 and its metabolites were analyzed in healthy animals after oral administration. To this end, 50 mg/kg of BTZ-043 was given orally to four guinea pigs. As shown in Fig. 1A, BTZ-043 (M0) reached a maximum plasma level of 1,442 ng/mL in one animal (peak; mean, 1,205 ng/mL after 1 h). The levels of the main amino-metabolite (M1) were very low over the entire testing period, with a maximum plasma level of 380 ng/mL in one guinea pig after 2 h (mean, 150 ng/mL). Since relevant levels were only reached for 2 h, additional doses, i.e., 200 mg/kg of either micronized or wet-milled BTZ-043 and 400 mg/kg of BTZ-043, were evaluated. The experiments were conducted in the same animals with a washout period of at least 7 weeks between treatments. After treatment with a dosage of 200 mg/kg (micronized), plasma levels of M0 peaked after 1 h (853 ng/mL) and of M1 after 2 h (1,851 ng/mL)

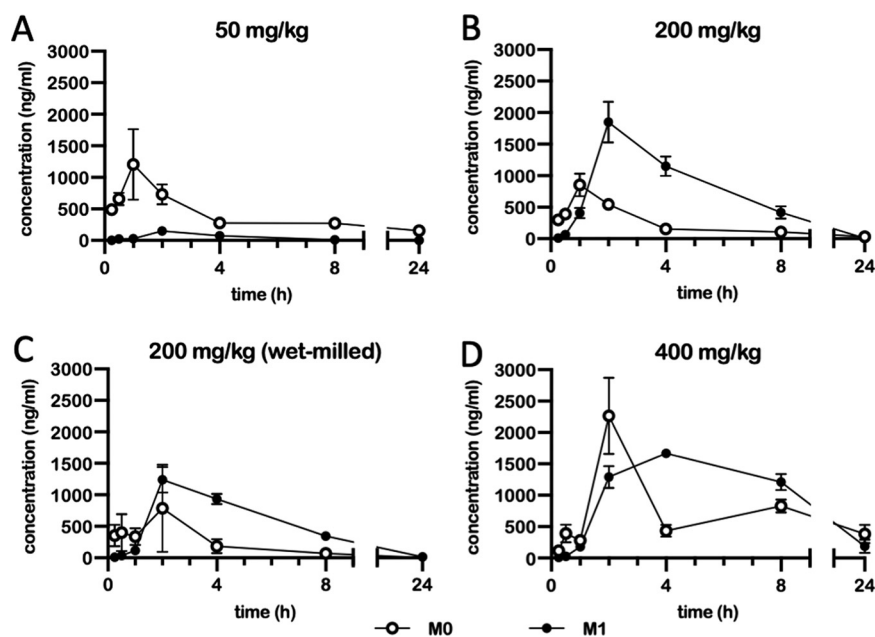


FIG 1 Plasma levels of BTZ-043 and its metabolite after oral BTZ-043 administration to guinea pigs. Four guinea pigs were given an oral dose of BTZ-043 (either 50 mg/kg, 200 mg/kg, or 400 mg/kg (all micronized) or 200 mg/kg (wet milled)). After 15 and 30 min and at 1, 2, 4, 8, and 24 h, blood was obtained from the vena saphena lateralis. The blood was centrifuged and plasma was separated into two samples, which were stabilized with ascorbic acid. After extraction, the samples were measured by mass spectrometry. The plasma levels of BTZ-043 (M0) and its metabolite M1 are shown for each time point as the group mean. Error bars represent the standard errors of the means.

but rapidly declined thereafter and reached baseline level after 24 h (Fig. 1B). For 200 mg/kg of wet-milled BTZ-043 the results were similar, but maximum plasma levels were lower, reaching 787 ng/mL for M0 and 1,237 ng/mL for M1 after 2 h (Fig. 1C). At a dosage of 400 mg/kg of BTZ-043, plasma levels finally remained elevated over 24 h (Fig. 1D). They peaked again after 2 h, with maximum levels of 2,265 ng/mL for M0 and 1,288 ng/mL for M1. Hence, 400 mg/kg was chosen as the appropriate dose for a longer treatment scheme (see also Table S2 in the supplemental material).

After multidose application of BTZ-043, plasma levels remained elevated after 24 h. To study the pharmacokinetics (PK) of BTZ-043 in guinea pigs after multidose application, six guinea pigs were treated orally with 400 mg/kg of BTZ-043 on 8 consecutive days (Fig. 2A). Plasma levels reached a concentration of 1,331 ng/mL for M0 and 2,147 ng/mL for M1 after 1 h and remained detectable over the first 24 h (Fig. 2B). On the last sampling day (Fig. 2C), samples taken prior to oral administration represent time zero. Metabolite levels were recorded in these samples as follows: M0, 1,391 ng/mL, and M1, 1,823 ng/mL. Metabolite concentrations peaked 1 h after treatment (M0, 2,176 ng/mL) or after 2 h (M1, 5,185 ng/mL) and remained over 1,000 ng/mL for the rest of the observation period, i.e., 1,171 ng/mL and 1,861 ng/mL for M0 and M1, respectively, after 24 h. During treatment weight gain was interrupted, but the animals regained weight at a normal rate immediately after treatment stopped (Fig. S1A).

High levels of BTZ-043 were reached in BCG-induced granulomas. To evaluate the tissue concentration of BTZ-043, six guinea pigs were inoculated subcutaneously with 1×10^3 CFU of BCG in the left and right axillary region each. After 28 days, small, palpable nodules had formed at the site of inoculation. Twenty-eight days after inoculation, guinea pigs were treated for 7 days with a daily oral dose of 400 mg/kg of BTZ-043 (Fig. 3A). During treatment, weight gain was slightly reduced (Fig. S1B). Afterwards, at day 35 post-inoculation, guinea pigs were euthanized to harvest BCG-induced injection site granulomas. In guinea pigs at early time points, BCG induces lesions very similar to those induced by virulent mycobacteria, but BCG can be processed under biosafety level 2 (BSL2) conditions. It was therefore possible to analyze granuloma specimens by mass spectrometry

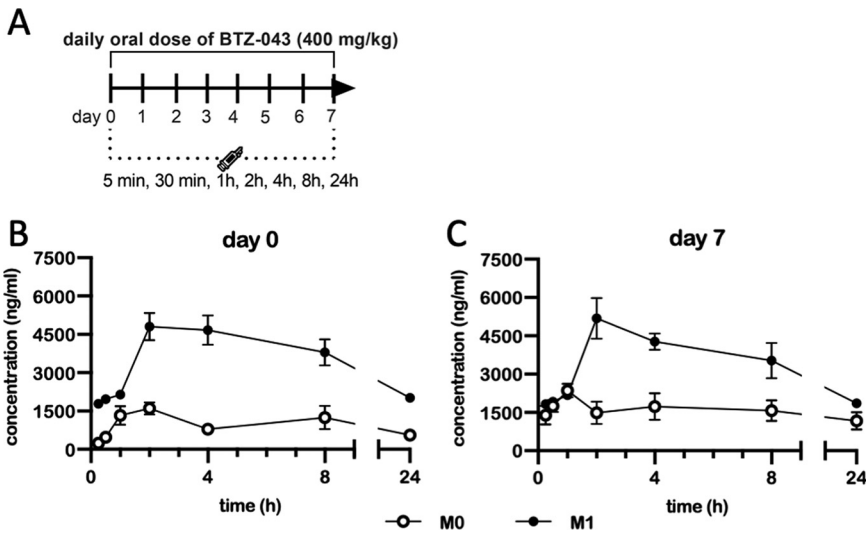


FIG 2 After multidose application of BTZ-043, plasma levels remained elevated after 24 h. (A) Six guinea pigs were given repeated single daily oral doses of 400 mg/kg of BTZ-043 over 7 consecutive days. On the first and last day, blood was obtained from the vena saphena lateralis at 15 and 30 min and at 1, 2, 4, 8, and 24 h after administration. The blood was centrifuged and plasma was separated into two samples, which were stabilized with ascorbic acid. After extraction, the samples were measured by mass spectrometry. The group mean of the plasma levels from BTZ-043 (M0) and its metabolite (M1) for each time point is shown for day 1 (B) and day 7 (C). Error bars represent the standard errors of the means.

under native conditions. BTZ-043 and its metabolite M1 were measured in relatively high concentrations compared to plasma levels (M0, 6,743 ng/g; M1, 8,768 ng/g) within granulomas. (Fig. 3B). In BTZ-043-treated animals, CFU counts in BCG granulomas were reduced by two log scales compared to those in untreated guinea pigs (Fig. 3C).

BTZ-043 treatment significantly reduced *M. tuberculosis*-induced pathology. Eighteen guinea pigs were infected subcutaneously in the left axillary region with 1×10^3 CFU of the virulent *M. tuberculosis* strain H37Rv. Fourteen days after infection, oral treatment was initiated and continued for the next 28 days (Fig. 4A). During repeated dosing

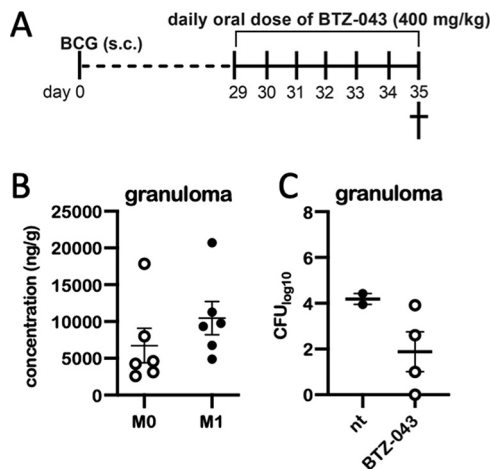


FIG 3 High levels of BTZ-043 are reached in BCG-induced granulomas. (A) Six guinea pigs were inoculated subcutaneously with 1×10^6 CFU of BCG Pasteur 1173. After 28 days, treatment with a daily oral dose of 400 mg/kg of BTZ-043 was started and continued for 7 consecutive days. At day 35, guinea pigs were euthanized and BCG-induced granulomas at the injection site were taken for analysis. (B) Parts of granulomas were cryopreserved and levels of BTZ-043 (M0) and its metabolite (M1) were measured via mass spectrometry. Individual levels and the means of M0 and M1 are shown for each of the six animals. Error bars represent the standard errors of the means. (C) For four treated animals, parts of granulomas were homogenized, serially diluted, and plated on 7H11 agar plates. After 3 weeks, CFU were counted. Results from two additional guinea pigs that were inoculated with BCG but not treated (nt) are depicted for comparison.

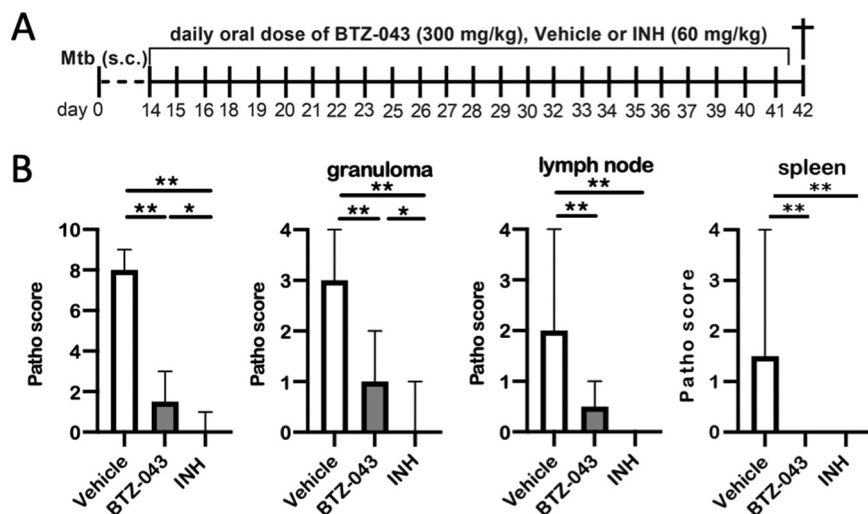


FIG 4 BTZ-043 treatment significantly reduced *M. tuberculosis*-induced pathology. (A) Guinea pigs ($n = 6$, each) were infected subcutaneously with 1×10^3 CFU of virulent *M. tuberculosis* strain H37Rv. After 14 days, treatment with a daily oral dose of 300 mg/kg of BTZ-043 was started and continued for 28 days. As a control, guinea pigs were treated with either vehicle solution or 60 mg/kg of isoniazid (INH). (B) After 4 weeks, guinea pigs were euthanized and necropsied. Granulomas at the infection site, the draining axillary lymph node, and spleen were macroscopically scored. Bars represent the group medians with ranges, and asterisks represent the level of significance as calculated by nonparametric Mann-Whitney U test (*, $P \leq 0.05$; **, $P \leq 0.01$).

of 400 mg/kg (in noninfected animals; see above), transient neurological signs such as tumbling or stupor were observed in some animals. Therefore, for the challenge trial, a dosage of 300 mg/kg of BTZ-043 was used. Vehicle-treated (1% carboxymethyl cellulose [CMC], 0.5% Tween 80) animals served as negative controls and isoniazid-treated (60 mg/kg) animals as positive controls. INH dosage was adapted from a previous publication (23). BTZ-043-treated animals showed the lowest weight gain in comparison to both control groups (Fig. S1C). At day 42, guinea pigs were euthanized and necropsied. The gross pathology scores of infection site granulomas, left axillary lymph nodes, and spleens were calculated. In comparison to those of vehicle-treated controls, the number and size of granulomas at the infection site and in the draining axillary lymph nodes was significantly reduced in BTZ-043- and INH-treated animals. Systemic spread, as determined by granulomatous splenitis, was completely absent in these two groups (Fig. 4B). Microscopic analysis of hematoxylin-eosin (HE)-stained tissue sections of the infection sites revealed that the size of granulomas (as determined by the absolute area in representative sections) and the percentage of necrosis within were significantly reduced in BTZ-043-treated guinea pigs in comparison to the vehicle group (Fig. 5A). Similar findings were evident in the draining axillary lymph nodes (Fig. 5B). For the spleen, granulomas were only detectable in animals of the vehicle control group (Fig. 5C). In infection site granulomas of BTZ-043-treated animals, slightly lower macrophage and higher T-cell counts were present than for vehicle- or INH-treated animals (Fig. S3A); this tendency did not reach significance. A similar nonsignificant trend was observed in draining axillary lymph nodes. Interestingly, in the lymph node, BTZ-043-treated animals showed 10-fold-higher numbers of B cells in the granulomatous region (Fig. S3B).

BTZ-043 treatment led to a significantly lower burden of virulent *M. tuberculosis* H37Rv. After 4 weeks of treatment, CFU of virulent *M. tuberculosis* H37Rv were determined at the site of infection, in the draining lymph node, and in the spleen. Compared to vehicle controls, significantly lower mycobacterial loads were observed at the site of infection in BTZ-043- and INH-treated animals (Fig. 6A). This reduction was even more striking in the lymph nodes (Fig. 6B). In contrast to vehicle controls in BTZ-043- or INH-treated guinea pigs, no mycobacteria were detectable in the spleen (Fig. 6C). Accordingly, when we analyzed additional organ samples outside the primary complex consisting of infection site granuloma and draining axillary lymph node, only

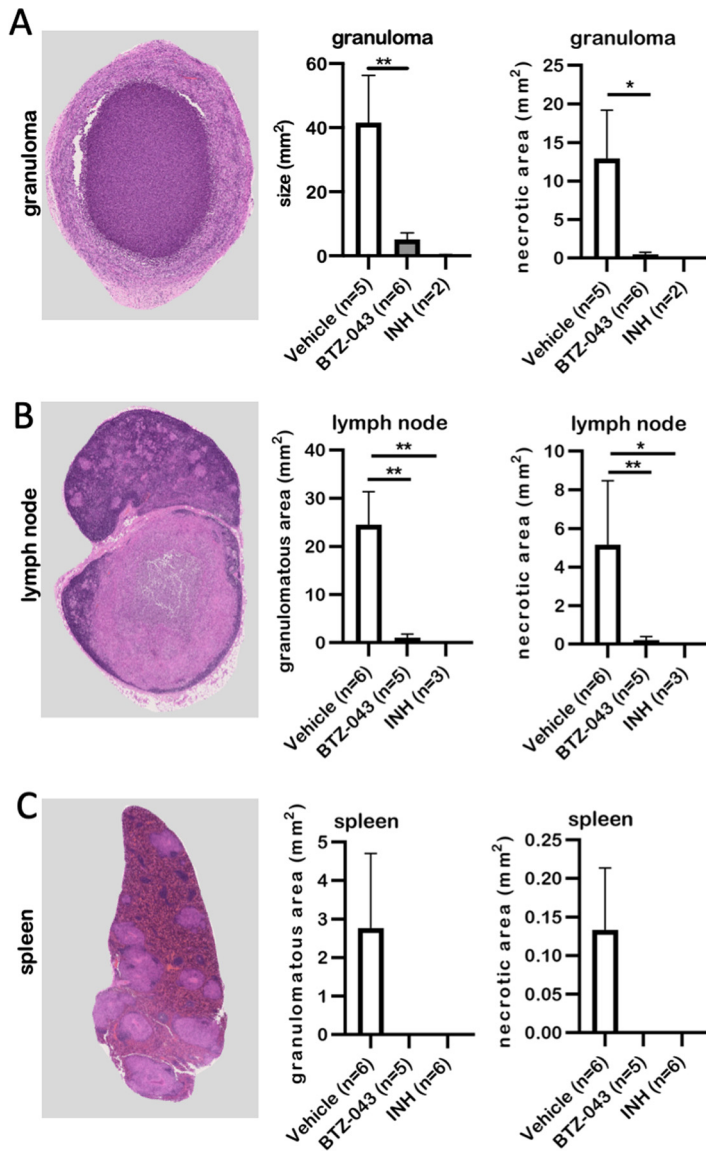


FIG 5 BTZ-043 treatment significantly reduced *M. tuberculosis*-induced necrotic lesions. Six weeks after infection and after 4 weeks of treatment, BTZ-043-treated or control animals (vehicle or INH) were euthanized and dissected and organ samples were collected. Formalin-fixed, paraffin-embedded sections of the infection site granuloma (A), the axillary lymph node (B), and the spleen (C) were HE stained, whole-slide images were obtained, and absolute granuloma areas as well as area of caseous necrosis were measured. Representative microphotographs for the respective organ are shown on the left. In the middle, the quantitative analysis of the granulomatous area is shown for the three groups. Graphs on the right depict the quantitative analysis of necrotic lesions. Bars show group means, error bars indicate the standard errors of the means, and asterisks indicate the level of significance as calculated by nonparametric Mann-Whitney U test (*, $P \leq 0.05$; **, $P \leq 0.01$).

in vehicle controls could lesions be detected: two out of six (33%) animals in the vehicle group had moderate, multifocal granulomas in the lymphonodus tracheobronchialis and mild, oligofocal, periportal centered granulomas in the liver of one animal. In the granulomas of the lung lymph node, single to a few acid-fast mycobacteria were visible (Fig. S2C to F).

DISCUSSION

In the middle of the 20th century, the discovery of antibiotics active against mycobacteria was an important turning point in the battle against TB (4). Uncountable numbers of deaths and severe TB cases could be averted through these new medications.

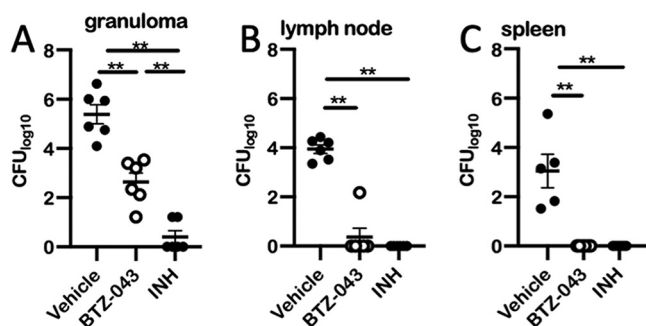


FIG 6 BTZ-043 treatment significantly reduced burden of virulent *M. tuberculosis* H37Rv. Six weeks after infection with virulent *M. tuberculosis* H37Rv, BTZ-043-treated or control animals (vehicle or INH) were euthanized and dissected and organ samples were obtained. Tissue samples of injection site granulomas (A), draining axillary lymph nodes (B), and the spleen (C) were homogenized and the number of CFU determined. Dots represent individual values for each animal. Black bars represent the group means and error bars the standard errors of the means. Asterisks show level of significance as calculated by nonparametric Mann-Whitney U test (**, $P \leq 0.01$).

However, since the 1990s, multidrug-resistant TB-causing strains have gained increasing relevance. In 2021, approximately 7% of all culture-confirmed cases worldwide were RR- or MDR-TB (1). Patients with MDR-TB need prolonged courses of treatment with a complicated treatment regimen involving several second-line drugs. This leads to more severe adverse effects and up to 100-fold-higher expenditures compared to those for drug-sensitive TB cases (24). The urgent need for new drugs that are as efficient and cost-effective as current first-line antibiotics has bolstered research and development efforts across academia, pharmaceutical companies, and public-private partnerships. A recent encouraging review gives a comprehensive overview over the pipeline of investigational drugs that are already approved or in clinical phase trials (25). One of these promising compounds is BTZ-043. Makarov et al. observed that BTZ-043 had very good activity against the different *M. tuberculosis* strains tested, including MDR and XDR strains (12). Furthermore, the *in vitro* MIC was found to be lower than those of other antimycobacterial drugs (26). In several animal models, oral administration of BTZ-043 yielded detectable plasma levels, with doses varying from 5 mg/kg to 300 mg/kg BTZ-043 in mice (12, 16) and 60 to 470 mg/kg in rats (15; unpublished data) and at up to 2,000 mg/kg BTZ-043 in minipigs (unpublished data). Although after single doses the levels rapidly decline over 24 h, good antimicrobial activity was observed in the mouse infection model (12). However, one general concern with the BALB/c mouse model is that mice normally do not develop caseating granulomas upon infection with *M. tuberculosis*. The aim of the current study was therefore to establish a preclinical model that would allow studying granuloma penetration and the effect of BTZ-043 on granuloma resident mycobacteria. As goats and cattle develop caseating granulomas and, like humans, have interlobular lung septa that help to encapsulate mycobacterial lesions, they have been proposed as experimental models to study the pathobiology of granuloma formation (27). However, by oral and even intravenous administration of BTZ-043 no detectable plasma levels of BTZ-043 could be reached in goats (unpublished data). We therefore made use of another preclinical TB model: guinea pigs, which have been used since the early days of TB research (28). They are highly susceptible to mycobacterial infections and develop granulomas very similar to those seen in human TB patients (22). In the current study, we were able to confirm that oral administration of BTZ-043 to guinea pigs resulted in plasma levels that were very similar to those reported for mice (12). With the maximum dose of 400 mg/kg, some of the adolescent animals in the multi-dose study developed transient, mild neurological symptoms. Adolescent animals are likely to be particularly susceptible to such side effects due to low adipose tissue levels resulting in differential drug distribution. In older animals receiving the high-dose bolus, no adverse effects were observed. Similarly, when the reduced dose of 300 mg/kg was applied in the treatment and challenge trial, no neurological symptoms occurred. In the

ongoing clinical trial, particular attention will be paid to potential adverse reactions. However, in relation to the metabolic weight, the highest dosage in the clinical trial is 5-fold lower than the dosage used in guinea pigs (21). Therefore, the occurrence of neurological symptoms is unlikely.

In the current study, we could for the first time directly determine the concentration of the active compound in *mycobacterium*-induced granulomas. Our observations in BCG-inoculated animals indicate that the compound is enriched in the granuloma, as the concentration in the tissue homogenates was about 7-fold higher than the corresponding plasma levels. This indicates that BTZ-043 is able to penetrate mature granulomas, reaching tissue levels that are clearly higher than the MIC. The M1 metabolite is the nitroreduction product of BTZ-043. Its MIC (500 ng/mL) is orders of magnitude higher than that of BTZ-043 (1 ng/mL) (12). However, the tissue levels of M1 in the granuloma suggest that it also contributed to antimicrobial activity. A fine differentiation of tissue concentrations, as has been described for moxifloxacin in lung granulomas of TB-infected rabbits (29), was beyond the scope of our study. However, as revealed by Ziehl-Neelsen staining in TB-infected vehicle controls, most acid-fast mycobacteria were observed extracellularly in the necrotic, caseous area of the granulomas (see Fig. S2 in the supplemental material). Hence, the significant reduction of the bacterial burden in BTZ-043-treated animals compared to vehicle controls—both in BCG-vaccinated animals and after virulent *M. tuberculosis* challenge—provides additional, indirect evidence that the active compound reached poorly vascularized areas, where the mycobacteria reside. This reduction of bacterial burden at the site of infection and in the draining axillary lymph node and the complete prevention of bacterial dissemination by BTZ-043 treatment were the most important outcomes of this study. While all animals of the vehicle control group had multiple granulomas in the spleen, and some showed lesions in the lung lymph nodes and liver, no lesions whatsoever were observed outside the primary complex in treated animals. This went along with significantly reduced macroscopic granuloma scores at the site of infection and in the draining lymph nodes. Also, at the microscopic level, this was reflected by significantly smaller granulomas and an almost complete absence of necrotic lesions in BTZ-043-treated animals. The immunophenotyping showed a nonsignificant increase in absolute T-cell counts in the infection site granuloma and in granulomatous areas of the lymph node in BTZ-043-treated animals in comparison to vehicle controls (Fig. S3). This nonsignificant trend is clearly no proof of an immunostimulatory effect of BTZ-043. However, the mere possibility of a complementary, immune-enhancing effect should be investigated in more detail, because other antimycobacterial drugs, such as rifampicin and INH, have been described to have a dampening effect on antimycobacterial immune responses (30, 31).

In our hands with the 28-day treatment regimen, INH had a better effect than BTZ-043. This observation is in line with previous studies from Lechartier et al. and Makarov et al., in which INH also showed a slightly better *in vitro* (18) and *in vivo* (17) efficacy than BTZ-043. At the same time, in a large European study including 240 clinical isolates, all tested INH-resistant *M. tuberculosis* isolates proved uniformly susceptible to BTZ-043 (20). Hence, in cases of MDR-TB, BTZ-043 is expected to be as effective as with drug-sensitive strains. In addition, work is ongoing to enhance the efficacy of BTZ-043: in a recent, so-far-unpublished study in BALB/c mice, 4-fold-higher plasma levels of BTZ-043 were achieved compared to those in previous mouse studies. Together with a prolonged treatment, this resulted in substantially higher killing rates after BTZ-043 than after INH treatment (unpublished data). Along that line, Makarov et al. already pointed out in their first, seminal publication that the efficacy of BTZ-043 is dependent on the duration of therapy rather than on the actual dose (12). So, with 28 days of treatment a highly significant and convincing therapeutic effect was observed, but it can be expected that prolonged therapy will further enhance the antimycobacterial effect of BTZ-043.

In summary, we have shown that the guinea pig is well suited to study the pharmacodynamics and pharmacokinetics of BTZ-043. The model is available to test the

compound in combination therapies with first-line drugs, such as INH or rifampicin (18), or to evaluate new derivatives of BTZ-043 (32–34). Most importantly, our current study unequivocally shows that BTZ-043 is able to penetrate the TB granuloma and that the treatment of *M. tuberculosis*-infected guinea pigs is safe and highly effective.

MATERIALS AND METHODS

Treatment. The benzothiazinone BTZ-043 (for detailed information, see Table S1 in the supplemental material) was administered as microcrystalline suspensions (micronized material or obtained through wet milling) in 1% carboxymethyl cellulose (CMC; medium viscosity) and 0.5% Tween 80 (Sigma-Aldrich, Germany). The amount of BTZ-043 in the formulation depended on the dosage (constant dosing volumes of 2 g/kg). In the dose-finding study, different doses and formulations were tested to establish the most effective dose. Hence, guinea pigs were treated with 50 mg/kg, 200 mg/kg, and 400 mg/kg (micronized). A comparison with a wet-milled formulation was done for the 200-mg/kg dose. For the multidose application and the BCG treatment study, a dose of 400 mg/kg (micronized) of BTZ-043 was used, and for the treatment after *M. tuberculosis* infection, a dose of 300 mg/kg (micronized) of BTZ-043 was used. The medication was stirred half an hour prior to each application for optimal homogeneity.

Isoniazid (INH), formulated with 30 mg/g in sterile water, at a dose of 60 mg/kg served as a positive control (23). As a negative control, a vehicle solution with 1% CMC and 0.5% Tween 80 was used.

Bacteria. For infection of guinea pigs, *Mycobacterium bovis* BCG strain Pasteur 1173 (kindly provided by Walter Mattheis, Paul-Ehrlich-Institut [PEI], Langen, Germany) or the *M. tuberculosis* H37Rv strain (kindly provided by Stefan H. E. Kaufmann, Max-Planck-Institute for Infection Biology, Berlin, Germany) was used. Bacteria were grown in oleic acid-albumin-dextrose-catalase (OADC)-enriched 7H9 medium (Becton, Dickinson, Germany) supplemented with 0.05% Tween 80 (Sigma-Aldrich, Germany). When grown to an optical density (OD) of 1.0, they were centrifuged and diluted in phosphate-buffered saline (PBS; in-house) for subcutaneous injection into guinea pigs.

Animal experiments. A total number of 34 3-month-old female Dunkin-Hartley guinea pigs were obtained from Charles River Germany and housed in groups of 2 or 3 animals. The guinea pigs were housed in open cages in the institute's biosafety level 2 or 3 animal facilities. Dry pellets, hay, and water were offered *ad libitum*; the light regime followed a natural day and night cycle and temperature was regulated automatically to 21°C. The cages were enriched with a plastic shelter and paper tunnels. Before the trial, animals were able to adjust to housing and handling during an acclimatization phase of 2 weeks. Animals were weighed weekly during the acclimatization period and daily during multidose studies.

The animal trial protocol was approved by the regulatory authority, the State Office of Agriculture, Food Safety and Fishery in Mecklenburg-Western Pomerania (LALLF MV, 7221.3-1-008/20). All animal experiments were carried out following German animal welfare regulations.

Experimental design. (i) Dose-finding study. In a dose-finding study, four guinea pigs were first given 50 mg/kg of BTZ-043 orally. After an appropriate resting and washout phase of at least 7 weeks in between, escalating doses of 200 mg/kg and 400 mg/kg were administered to the same animals. Following oral application of BTZ-043, blood was obtained from the vena saphena lateralis after 15 and 30 min and at 1, 2, 4, 8, and 24 h. Measurement of plasma concentrations was conducted as described below.

(ii) Multidose application. Six guinea pigs were given 400 mg/kg of BTZ-043 orally for 8 consecutive days. On the first and last day, blood was obtained as described above and bioanalysis was done as described below.

(iii) BTZ-043 in granulomas. Six animals were injected subcutaneously with a dose of 1×10^3 CFU of BCG strain Pasteur 1173 resuspended in 0.25 mL of PBS. Equal amounts of this injection suspension were administered in the left and the right axillary region to induce granuloma formation on each side. After 28 days, 400 mg/kg of BTZ-043 was given orally once daily for 7 consecutive days. On day 35, guinea pigs were euthanized by CO₂ inhalation under deep anesthesia using ketamine (Livisto, Germany) and xylazine (CP-Pharma, Germany). Injection site granulomas were collected and split into equal parts for bacteriology and BTZ-043 concentration determination. CFU were determined as described for *M. tuberculosis*-challenged animals (see below).

(iv) BTZ-043 after *M. tuberculosis* infection. Eighteen guinea pigs were infected subcutaneously with 1×10^3 CFU of virulent *M. tuberculosis* strain H37Rv in the left axillary region. After 14 days, treatment was started and given once daily for 28 consecutive days. One group of six animals received a daily oral dose of 300 mg/kg of BTZ-043. As a positive control, six guinea pigs were given 60 mg/kg of INH, and as a negative control, six animals received vehicle solution. After 28 days of treatment, i.e., 42 days after inoculation, guinea pigs were euthanized and necropsied. Tissue samples were collected for further bacteriological and histological analyses (see below).

Sample workflow for BTZ-043 bioanalysis. (i) Sample preparation. Immediately after blood withdrawal from the vena saphena, the blood was stored on ice and quickly centrifuged at 1,600 relative centrifugal force (rcf) for 10 min at 4°C. The plasma was then separated in duplicates and stabilized with ascorbic acid (2.5 mg/mL). Injection site granulomas from the guinea pigs were immediately cryopreserved and kept frozen at –80°C until analysis.

(ii) Pretreatment for plasma samples. Aliquots of 10 μ L were mixed with 10 μ L of ascorbic acid solution (250 mg/mL in deionized water), 10 μ L of internal standard (IS) (800 ng/mL in methanol (MeOH)), and 70 μ L of degassed MeOH. After mixing for 2 min using an Eppendorf ThermoMixer C at 4°C and centrifugation at 16,100 rcf for 2 min at 4°C, supernatants were taken immediately for quantification.

(iii) Pretreatment for granuloma samples. Prior to homogenization of granuloma tissue samples from BCG-injected and BTZ-043-treated guinea pigs, a stability test was performed to ascertain that BTZ-043 and its main metabolites did not degrade due to the heat created from homogenization beads. Blank granuloma tissue and the experimental granuloma tissue samples were homogenized in Precellys lysing kits CK14 (2 mL, pre-filled with ceramic beads; Bertin Technologies SAS, France) using a Precellys 24 tissue homogenizer (Bertin Technologies SAS). Tissue was accurately weighted, and 9-fold (wt/wt) PBS (Lonza, USA) was added. Instead of homogenizing tissue samples continuously for 60 s, the procedure was repeated 3 times by homogenizing the samples for 20 s at 5,500 rpm and intermediary cooling in an ice bath for 5 min to avoid overheating. Tissue homogenates were stored at -80°C until use. Additionally, a recovery test was performed on the granuloma homogenates by spiking BTZ-043 and its different metabolites into the tissue homogenization preparations. Recoveries were around 80 to 86%, validating the process of homogenization of granuloma samples.

Bioanalysis. (i) Stock and working solutions. Under physiological conditions, BTZ-043 (M0) is metabolized into (besides minor metabolites) its main metabolites M1 (amino-metabolite) and M2 (hydride Meisenheimer complex). M2 is unstable under atmospheric conditions and is prone to oxidize to the parent compound (BTZ-043) *ex vivo*, which can be suppressed through addition of ascorbic acid. As only M0 and, to a lesser extent, M1 are known to have antibacterial activity, we focused on these metabolites in Results.

(ii) Calibration and QC samples. Calibration and quality control (QC) samples were obtained by adding constant volumes of different analyte working dilutions (10 μL) into blank plasma (115 μL). The spiking was limited to a final solvent content maximum of 8% (vol/vol). The calibration standards and QC samples of the cocktail solution (M0 and M1) were prepared in blank plasma (stabilized with ascorbic acid at 2.5 mg/mL). See calibration standards and QC samples in Table S3.

(iii) Quantification of BTZ-043 and its main metabolites. Samples were analyzed using a Vanquish Horizon ultrahigh-performance liquid chromatography (UHPLC) system (Thermo Fisher Scientific, Germany) coupled to a Thermo Scientific QExactive HF-X Orbitrap mass spectrometer using a UPLC column (Acquity HSS T3; Waters; 1.8- μm particle size; 2.1 by 50 mm) and a precolumn (Acquity HSS T3 VanGuard precolumn; Waters; 1.8- μm particle size; 2.1 by 5 mm). The column temperature was maintained at 25°C , and the samples were kept at 4°C . The UHPLC system was operated at a flow rate of 0.6 mL/min and an injection volume of 5 μL . Mobile phases consisted of 0.1% (vol/vol) formic acid in water (eluent A) and 0.1% (vol/vol) formic acid in acetonitrile (ACN) (eluent B). Chromatographic separation was achieved as follows: 0 to 4 min, linear gradient from 5% to 98% eluent B; 4 to 6.5 min, isocratic at 98% eluent B; 6.5 to 7 min, linear gradient from 98% to 5% eluent B; and 7 to 9 min, isocratic at 5% eluent B. The high-resolution mass spectra were acquired with electrospray ionization in the positive mode. A scan range of m/z 120 to 1,800 was chosen, and the maximum injection time was set to 200 ms. Ion source parameters were as follows: spray voltage, 3.5 kV; capillary temperature, 320°C ; S-lens radiofrequency (RF) level, 40; sheath gas pressure, 50 ($\text{N}_2 > 95\%$); auxiliary gas pressure, 10 ($\text{N}_2 > 95\%$); and auxiliary gas heater temperature, 300°C . The value for the automatic gain control (AGC) target was set to 10^6 , resolution was 60,000, and chromatographic peak width (full width at half maximum [FWHM]) was 15 s. Samples were measured when good calibration curves of analytes and valid QC results were obtained. During analysis, ACN solution was injected after every four samples. QC samples were injected after a batch of 24 to 30 samples, as well as after all the samples. All the samples were measured within 6 h after the sample pretreatment and were stored at -80°C after the analysis.

Data analysis of BTZ-043 measurements. (i) Evaluation of analytical data. Chromatographic data were integrated and evaluated using the software TraceFinder (Thermo Fisher) with the following parameters: calculation method, peak area ratio; regression type, linear; weighting factor, $1/x^2$; and rounding of results, three significant figures.

Measured concentrations were listed and summarized for each sampling time point and animal by calculation of means and standard deviation per time point.

(ii) PK evaluation. The pharmacokinetic (PK) assessment was performed based on mean concentrations. The following PK parameters were determined by noncompartmental methods using Phoenix WinNonlin 7.0: maximum concentration (C_{max}), time to maximum concentration (T_{max}), area under the curve from 0 to t area under the curve over the observation period (AUC_{0-t}), calculated total area under the curve ($\text{AUC}_{0-\text{inf}}$), the proportion of the total AUC after the observation period (% $\text{AUC}_{\text{extra}}$), if applicable. Measured concentrations and PK parameters were summarized by group mean values and standard deviation. For T_{max} , the median was reported. All calculated parameters were rounded to three figures.

Necropsy and sampling of *M. tuberculosis*-infected guinea pigs. Forty-two days after *M. tuberculosis* infection and after 28 days of treatment, guinea pigs were euthanized under anesthesia (see above) with pentobarbital (Release; WDT, Germany) followed by a full necropsy. Samples from infection site, draining left axillary lymph node, and spleen were taken and used for bacterial cultivation and histopathological analysis. Heart, trachea, cranial and caudal lung lobe, lymphonodus tracheobronchialis, stomach, duodenum, jejunum, ileum, colon, liver, pancreas, kidney, and brain were additionally sampled for histopathological analysis. Samples for histopathology were immediately fixated in formaldehyde and after 3 weeks in paraffin wax-embedded (FFPE) tissue blocks. Samples for bacterial enumeration of CFU were homogenized and plated on the same day. Samples of tissues were split in equal parts for bacteriological and histopathological analyses. In cases where the samples were too small to perform both analyses, CFU determination was prioritized.

Macroscopic scoring of gross lesions was performed for the infection site, left axillary lymph node, and spleen by assessing formation of granulomas, number and size of granulomas, and presence of necrosis. The scores were derived from an ordinal scale of 0 to 4 based on the modified Mitchison scoring system detailed in Table S1 (35, 36).

Measurement of bacterial growth. Tissue samples from the injection site granuloma, draining left axillary lymph node, and spleen were diluted in 1 mL of PBS containing 0.05% Tween 80 (Sigma-Aldrich, Germany). Samples were homogenized and the homogenate was 1:10 serially diluted from 1:100 to 1:1,000,000. Fifty microliters of each solution was plated on 7H11 agar (Sigma-Aldrich, Germany) supplemented with 5 g/L of glycerin, 100 mL/L of OADC (Becton, Dickinson, Germany), and 500 μ L/L of ampicillin (Carl Roth, Germany). Agar plates were incubated at 37°C for 3 weeks before counting the number of CFU.

Microscopic analysis. (i) FFPE tissue preparation and histochemistry. FFPE tissues were cut at 3 μ m and hematoxylin-eosin (HE) as well as Ziehl-Neelsen or Fite-Faraco staining was performed to visualize acid-fast mycobacteria in granulomas according to standard laboratory protocols (37).

(ii) Immunohistochemistry. To visualize B cells, T cells, and macrophages, primary antibodies were used as described in Table S4. As secondary antibody, a biotinylated goat anti-mouse IgG (1:200; Vector Laboratories, Burlingame, CA; for CD79a) antibody was used with subsequent avidin-biotin-peroxidase (ABC) complex (Vector Laboratories) for 30 min at room temperature. For visualization of T cells and macrophages, the EnVision+ system (Dako, USA) was used.

(iii) Whole-slide image (WSI) analysis. The stained slides were scanned with a NanoZoomer S60 digital slide scanner (Hamamatsu, Germany) in 40 \times mode. For all digital analysis of the scanned slides, QuPath version 0.2.3. (38) was used.

As we prioritized assessment of CFU, in some animals there was not enough tissue left for microscopic analysis of infection site granulomas. The exact numbers of analyzed tissue samples are given in the respective figures for each treated group. The areas of organs as well as granulomatous and necrotic areas within granulomas were determined on HE-stained slides by WSI. Positive cells obtained in immunophenotyped consecutive sections were automatically enumerated with QuPath using the program cell detection algorithm (38). For each consecutive section, several visual fields representative for the area of tissue and granuloma were analyzed at a magnification of \times 400. For each immunophenotyped WSI, the detection parameters were adjusted and all analyses were manually supervised.

Statistics. GraphPad Prism version 8.1.0 was used to analyze and visualize the data. Differences at a *P* value of <0.05 were considered significant. Quantitative data are expressed as group means plus/minus standard errors of the means (SEM). Semiquantitative data (gross pathology scoring) are depicted as medians with ranges. The results between groups were compared using Mann-Whitney U test.

SUPPLEMENTAL MATERIAL

Supplemental material is available online only.

SUPPLEMENTAL FILE 1, PDF file, 12.6 MB.

ACKNOWLEDGMENTS

We thank Walter Mattheis and Stefan H. E. Kaufmann for the provision of bacterial strains. We are particularly grateful to Wiebke Lange, Silvia Schuparis, Gabriele Czerwinski, and Ulrike Zedler for their excellent technical support. We emphasize the contribution of Frank Klipp, Bärbel Bergmann, and all the animal care takers, and we sincerely acknowledge the help of Angele Breithaupt, Bärbel Hammerschmidt, and Charlotte Schröder.

We have no financial conflict of interest.

This study was funded by the Federal Ministry for Education and Research as part of the InfectControl Consortium (grant no. 03ZZ0803B for M.B., 03ZZ0803A and 03ZZ0835A for F.K., and 03ZZ0826 for Y.L.).

REFERENCES

- World Health Organization. 2021. Global tuberculosis report 2021. World Health Organization, Geneva, Switzerland.
- Lenaerts AJ, Degroote MA, Orme IM. 2008. Preclinical testing of new drugs for tuberculosis: current challenges. *Trends Microbiol* 16:48–54. <https://doi.org/10.1016/j.tim.2007.12.002>.
- Tandon R, Nath M. 2017. Tackling drug-resistant tuberculosis: current trends and approaches. *Mini Rev Med Chem* 17:549–570. <https://doi.org/10.2174/1389557516666160606204639>.
- Matteelli A, Roggi A, Carvalho AC. 2014. Extensively drug-resistant tuberculosis: epidemiology and management. *Clin Epidemiol* 6:111–118. <https://doi.org/10.2147/CLEP.S35839>.
- World Health Organization. 2020. Global tuberculosis report 2020. World Health Organization, Geneva, Switzerland.
- Evangelopoulos D, McHugh TD. 2015. Improving the tuberculosis drug development pipeline. *Chem Biol Drug Des* 86:951–960. <https://doi.org/10.1111/cbdd.12549>.
- Philips JA, Ernst JD. 2012. Tuberculosis pathogenesis and immunity. *Annu Rev Pathol* 7:353–384. <https://doi.org/10.1146/annurev-pathol-011811-132458>.
- Lange C, Aarnoutse R, Chesov D, van Crevel R, Gillespie SH, Grobbel H-P, Kalsdorf B, Kontsevaya I, van Laarhoven A, Nishiguchi T, Mandalakas A, Merker M, Niemann S, Köhler N, Heyckendorf J, Reimann M, Ruhwald M, Sanchez-Carballo P, Schwudke D, Waldow F, DiNardo AR. 2020. Perspective for precision medicine for tuberculosis. *Front Immunol* 11:566608. <https://doi.org/10.3389/fimmu.2020.566608>.
- Köser CU, Javid B, Liddell K, Ellington MJ, Feuerriegel S, Niemann S, Brown NM, Burman WJ, Abubakar I, Ismail NA, Moore D, Peacock SJ, Török ME. 2015. Drug-resistance mechanisms and tuberculosis drugs. *Lancet* 385: 305–307. [https://doi.org/10.1016/S0140-6736\(14\)62450-8](https://doi.org/10.1016/S0140-6736(14)62450-8).
- Shetye GS, Franzblau SG, Cho S. 2020. New tuberculosis drug targets, their inhibitors, and potential therapeutic impact. *Transl Res* 220:68–97. <https://doi.org/10.1016/j.trsl.2020.03.007>.
- Vilchèze C. 2020. Mycobacterial cell wall: a source of successful targets for old and new drugs. *Appl Sci* 10:2278. <https://doi.org/10.3390/app10072278>.
- Makarov V, Manina G, Mikusova K, Möllmann U, Ryabova O, Saint-Joanis B, Dhar N, Pasca MR, Buroni S, Lucarelli AP, Milano A, de Rossi E, Belanova M, Bobovska A, Dianiskova P, Kordulakova J, Sala C, Fullam E, Schneider P, McKinney JD, Brodin P, Christophe T, Waddell S, Butcher P, Albrethsen J,

- Rosenkrands I, Brosch R, Nandi V, Bharath S, Gaonkar S, Shandil RK, Balasubramanian V, Balganesht T, Tyagi S, Grosset J, Riccardi G, Cole ST. 2009. Benzothiazinones kill Mycobacterium tuberculosis by blocking arabinan synthesis. *Science* 324:801–804. <https://doi.org/10.1126/science.1171583>.
13. Trefzer C, Škovierová H, Buroni S, Bobovská A, Nenci S, Molteni E, Pojer F, Pasca MR, Makarov V, Cole ST, Riccardi G, Mikušová K, Johnsson K. 2012. Benzothiazinones are suicide inhibitors of mycobacterial decaprenylphosphoryl- β -D-ribofuranose 2'-oxidase DprE1. *J Am Chem Soc* 134:912–915. <https://doi.org/10.1021/ja211042r>.
 14. Neres J, Pojer F, Molteni E, Chiarelli LR, Dhar N, Boy-Röttger S, Buroni S, Fullam E, Degiacomi G, Lucarelli AP, Read RJ, Zannoni G, Edmondson DE, de Rossi E, Pasca MR, McKinney JD, Dyson PJ, Riccardi G, Mattevi A, Cole ST, Binda C. 2012. Structural basis for benzothiazinone-mediated killing of Mycobacterium tuberculosis. *Sci Transl Med* 4:150ra121. <https://doi.org/10.1126/scitranslmed.3004395>.
 15. Gao C, Peng C, Shi Y, You X, Ran K, Xiong L, Ye T, Zhang L, Wang N, Zhu Y, Liu K, Zuo W, Yu L, Wei Y. 2016. Benzothiazinethione is a potent preclinical candidate for the treatment of drug-resistant tuberculosis. *Sci Rep* 6: 29717. <https://doi.org/10.1038/srep29717>.
 16. González-Martínez NA, Lozano-Garza HG, Castro-Garza J, de Osio-Cortez A, Vargas-Villareal J, Cavazos-Rocha N, Ocampo-Candiani J, Makarov V, Cole ST, Vera-Cabrera L. 2015. In vivo activity of the benzothiazinones PBTZ169 and BTZ043 against *Mycobacterium tuberculosis*. *PLoS Negl Trop Dis* 9: e0004022. <https://doi.org/10.1371/journal.pntd.0004022>.
 17. Makarov V, Lechartier B, Zhang M, Neres J, van der Sar AM, Raadsen SA, Hartkoorn RC, Ryabova OB, Vocat A, Decosterd LA, Widmer N, Buclin T, Bitter W, Andries K, Pojer F, Dyson PJ, Cole ST. 2014. Towards a new combination therapy for tuberculosis with next generation benzothiazinones. *EMBO Mol Med* 6:372–383. <https://doi.org/10.1002/emmm.201303575>.
 18. Lechartier B, Hartkoorn RC, Cole ST. 2012. In vitro combination studies of benzothiazinone lead compound BTZ043 against Mycobacterium tuberculosis. *Antimicrob Agents Chemother* 56:5790–5793. <https://doi.org/10.1128/AAC.01476-12>.
 19. Working Group for New TB Drugs. 2020. BTZ-043. <https://www.newtbdrugs.org/pipeline/compound/btz-043>. Accessed 22 February 2022.
 20. Pasca MR, Degiacomi G, Ribeiro ALdJL, Zara F, de Mori P, Heym B, Mirrione M, Brerra R, Pagani L, Pucillo L, Troupioti P, Makarov V, Cole ST, Riccardi G. 2010. Clinical isolates of Mycobacterium tuberculosis in four European hospitals are uniformly susceptible to benzothiazinones. *Antimicrob Agents Chemother* 54:1616–1618. <https://doi.org/10.1128/AAC.01676-09>.
 21. Hoelscher M. 2022. A prospective phase Ib/Ia, active-controlled, randomized, open-label study to evaluate the safety, tolerability, extended early bactericidal activity and pharmacokinetics of multiple oral doses of BTZ-043 tablets in subjects with newly diagnosed, uncomplicated, smear-positive, drug-susceptible pulmonary tuberculosis. <https://www.clinicaltrials.gov/ct2/show/NCT04044001>. Accessed 20 September 2022.
 22. Clark S, Hall Y, Williams A. 2014. Animal models of tuberculosis: guinea pigs. *Cold Spring Harb Perspect Med* 5:a018572. <https://doi.org/10.1101/cshperspect.a018572>.
 23. Ahmad Z, Klinckenberg LG, Pinn ML, Fraig MM, Peloquin CA, Bishai WR, Nuermberger EL, Grosset JH, Karakousis PC. 2009. Biphasic kill curve of isoniazid reveals the presence of drug-tolerant, not drug-resistant, Mycobacterium tuberculosis in the guinea pig. *J Infect Dis* 200:1136–1143. <https://doi.org/10.1086/605605>.
 24. Institute of Medicine Forum on Drug Discovery, Development, and Translation, Science, Russian Academy of Medical Science. 2011. The new profile of drug-resistant tuberculosis in Russia: a global and local perspective: summary of a joint workshop. National Academies Press, Washington, DC.
 25. Black TA, Buchwald UK. 2021. The pipeline of new molecules and regimens against drug-resistant tuberculosis. *J Clin Tuberc Other Mycobact Dis* 25:100285. <https://doi.org/10.1016/j.jctube.2021.100285>.
 26. da Silva PB, Campos DL, Ribeiro CM, da Silva IC, Pavan FR. 2017. New antimycobacterial agents in the pre-clinical phase or beyond: recent advances in patent literature (2001–2016). *Expert Opin Ther Pat* 27:269–282. <https://doi.org/10.1080/13543776.2017.1253681>.
 27. Liebler-Tenorio EM, Heyl J, Wedlich N, Figl J, Köhler H, Krishnamoorthy G, Nieuwenhuizen NE, Grode L, Kaufmann SHE, Menge C. 2022. Vaccine-induced subcutaneous granulomas in goats reflect differences in host-mycobacterium interactions between BCG- and recombinant BCG-derivative vaccines. *Int J Mol Sci* 23:10992. <https://doi.org/10.3390/ijms231910992>.
 28. Koch R. 1882. Die Ätiologie der Tuberkulose. *Berl Klin Wochenschr* 19:1–5. https://doi.org/10.1007/978-3-662-56454-7_5.
 29. Prideaux B, Dartois V, Staab D, Weiner DM, Goh A, Via LE, Barry CE, Stoeckli M. 2011. High-sensitivity MALDI-MRM-MS imaging of moxifloxacin distribution in tuberculosis-infected rabbit lungs and granulomatous lesions. *Anal Chem* 83:2112–2118. <https://doi.org/10.1021/ac1029049>.
 30. Kasik JE, Monick M, Thompson JS. 1976. Immunosuppressant activity of the ansamycins. *Antimicrob Agents Chemother* 9:470–473. <https://doi.org/10.1128/AAC.9.3.470>.
 31. Tousif S, Singh DK, Ahmad S, Moodley P, Bhattacharyya M, van Kaer L, Das G. 2014. Isoniazid induces apoptosis of activated CD4+ T cells: implications for post-therapy tuberculosis reactivation and reinfection. *J Biol Chem* 289:30190–30195. <https://doi.org/10.1074/jbc.C114.598946>.
 32. Richter A, Seidel RW, Goddard R, Eckhardt T, Lehmann C, Dörner J, Siersleben F, Sondermann T, Mann L, Patzer M, Jäger C, Reiling N, Imming P. 2022. BTZ-derived benzisothiazolinones with in vitro activity against Mycobacterium tuberculosis. *ACS Med Chem Lett* 13:1302–1310. <https://doi.org/10.1021/acsmchemlett.2c00215>.
 33. Madikizela B, Eckhardt T, Goddard R, Richter A, Lins A, Lehmann C, Imming P, Seidel RW. 2021. Synthesis, structural characterization and antimycobacterial evaluation of several halogenated non-nitro benzothiazinones. *Med Chem Res* 30:1523–1533. <https://doi.org/10.1007/s00044-021-02735-4>.
 34. Liu L, Kong C, Fumagalli M, Savková K, Xu Y, Huszár S, Sammartino JC, Fan D, Chiarelli LR, Mikušová K, Sun Z, Qiao C. 2020. Design, synthesis and evaluation of covalent inhibitors of DprE1 as antitubercular agents. *Eur J Med Chem* 208:112773. <https://doi.org/10.1016/j.ejmech.2020.112773>.
 35. Mitchison DA, Wallace JG, Bhatia AL, Selkon JB, Subbaiah TV, Lancaster MC. 1960. A comparison of the virulence in guinea-pigs of South Indian and British tubercle bacilli. *Tubercle* 41:1–22. [https://doi.org/10.1016/s0041-3879\(60\)80019-0](https://doi.org/10.1016/s0041-3879(60)80019-0).
 36. Jain R, Dey B, Dhar N, Rao V, Singh R, Gupta UD, Katoch VM, Ramanathan VD, Tyagi AK. 2008. Enhanced and enduring protection against tuberculosis by recombinant BCG-Ag85C and its association with modulation of cytokine profile in lung. *PLoS One* 3:e3869. <https://doi.org/10.1371/journal.pone.0003869>.
 37. Mulisch M, Welsch U. 2015. *Romeis-Mikroskopische Technik*. Springer, Berlin, Germany.
 38. Bankhead P, Loughrey MB, Fernández JA, Dombrowski Y, McArt DG, Dunne PD, McQuaid S, Gray RT, Murray LJ, Coleman HG, James JA, Salto-Tellez M, Hamilton PW. 2017. QuPath: open source software for digital pathology image analysis. *Sci Rep* 7:16878. <https://doi.org/10.1038/s41598-017-17204-5>.